A scalable integrated solar device for the autonomous production of green methane

Angela Maragno, Gregory Cwicklinski, Muriel Matheron, Romain Vannoorenberghe, Jean-Marc Borgard, Adina Morozan, Jennifer Fize, Michel Pellat, Christine Cavazza, Vincent Artero, et al.

A scalable integrated solar device for the autonomous production of green methane

Angela R. A. Maragno[1], Grégory Cwicklinski[2*], Muriel Matheron[3*†], Romain Vanoorenberghe[2], Jean-Marc Borgard[4], Adina Morozan[2], Jennifer Fize[2], Michel Pellat[5], Christine Cavazza[2], Vincent Artero[2], Sophie Charton[1,6*]

[1] CEA, DES, ISEC, DMRC, Univ. Montpellier, Marcoule, France
[2] Univ. Grenoble Alpes, CNRS, CEA, IRIG, Laboratoire de Chimie et Biologie des Métaux, 38000 Grenoble, France
[3] Univ. Grenoble Alpes, CEA, LITEN, Campus INES, 73375 Le Bourget du Lac, France
[4] CEA, DES, ISAS, DRMP, Univ. Paris-Saclay, 91191 Gif-sur-Yvette, France
[5] Univ. Grenoble Alpes ,CEA, DRT, LITEN, DTNM, 38000 Grenoble, France
[†] Present address: Univ. Grenoble Alpes, CEA, LITEN, DTCH, 38000 Grenoble, France

[6] Lead contact

*Correspondence : sophie.charton@cea.fr (S.C.)
muriel.matheron@cea.fr (M.M.)
gregory.cwicklinski@cea.fr (G.C.)

Summary

The solar-driven conversion of CO_2 into molecules with high calorific value is a major challenge to reduce the carbon footprint of industrialized countries. Many concepts are proposed, but limited action has been so far undertaken to design, integrate, and scale commercially viable technologies. Here we report on the long-term performance of an autonomous solar-driven device that converts continuously, under mild conditions, CO_2 into CH_4. It couples a biomethanation reactor to a set of integrated photo-electrochemical cells combining silicon / perovskite tandem solar cells with proton exchange membrane electrolysers, for the production of solar hydrogen from water. The 5.5 % solar to fuel yield (calculated from global horizontal irradiance) achieved by the bench-scale device during 72 hours of outdoor operation at JRC Ispra, Italy, in July 2022, demonstrates that re-design and close integration of proven lab-scale concepts can overcome the technological barriers to the industrial deployment of artificial photosynthesis process.

Introduction

The demand for sustainable and clean energy technologies has intensified over recent decades and is at the heart of the transition to an energy system less dependent on fossil fuels. Solar fuels, which harness the abundant and renewable energy from the sun to produce storable and transportable energy carriers, offer a promising solution to address these challenges. Despite significant progress in solar fuel technologies[1], the transition from laboratory-scale experiments to practical, scalable, and economically viable systems remains a critical area of research and only few prototypes have been demonstrated that can efficiently generate solar fuels under real-life conditions[2,3].

Methane, the primary component of natural gas, holds great potential as a solar fuel due to its high specific energy, wide use, and established infrastructure for storage and

distribution. Solar methane, as biomethane and synthetic methane, has a major role to play on the energy transition, by reducing both the need for natural gas in domestic or industrial usages and fossil fuels in transportation. The direct electrocatalytic conversion of CO_2 into valuable molecules, such as methane, is still challenging and exhibits poor performances both energetically and in terms of selectivity and conversion yield[4]. Today, the most energetically favorable process to transform CO_2 into synthetic CH_4 is the Sabatier reaction:

$$4\ H_2 + CO_2 = CH_4 + 2\ H_2O \qquad \text{(Equation 1)}$$

This reaction has aroused a great interest in the framework of Power-to-Gas technologies[5,6]. It requires significant excess of H_2, that is generally supplied by alkaline electrolysis, connected to the electrical grid. Alkaline electrolysis is among the most mature water electrolysis technology, knowing water electrolysis has a low CO_2 footprint only if coupled to renewable sources of electricity. Alternatively, solar hydrogen can be used to feed the Sabatier reaction with low overall environmental footprint. Among the many different technologies investigated during the last decades to produce solar hydrogen[8], photo-electrochemical (PEC) cells combine the versatility of electrochemical devices for water splitting to the light harvesting and charge separation properties of semiconductor materials. Techno-economic analysis shows that solar H_2 production from PEC technology could become competitive by 2050[9,10]. However, to reach maturity, such technologies should be at the same time efficient in terms of solar-to-hydrogen (STH) conversion efficiency, stable over years under intermittent operation, and scalable, which means that they should rely on Earth-abundant materials and cost- and energy-effective processes[11]. This will also require a substantial integration effort[12] to ensure optimized management of charge and heat,[13,14] mass transfer, as well as the safe management of large H_2 and O_2 amounts. Currently, the most efficient photovoltaic-driven electrolysis systems, with up to 30 % STH, rely on expensive III-V/Si multijunctions under concentrated light, associated to platinum-group metal based electrolysers[15–17]. Alternatively, integrated photoelectrochemical approaches that intimately couple photovoltaic cells to electrolysers (designated as IPEC, following the denomination proposed by Haussener[18]) have reached efficiencies up to 10% STH[18] (and see Fig. 21a in ref.[19]).

The direct coupling of solar H_2 production with the Sabatier reaction has never been investigated. Actually, the Sabatier reaction is a balanced exothermic reaction ($\Delta_r H^0 = -165$ kJ.mol^{-1}) which is industrially implemented in catalytic plug flow reactors, that operate at steady-state, elevated temperature (600 to 700 K), and with precise process control to minimize power demand, and guarantee high selectivity and efficiency of the catalyst. These conditions are hardly compatible with an intermittent supply of H_2, as delivered by stand-alone PEC cells, unless the process contains a hydrogen storage tank acting as a buffer for continuous hydrogen supply. Alternately, anaerobic methanogens are able to convert CO_2 into CH_4 under mild conditions of pressure and temperature. Eq. (1) is *de facto* part of the metabolism of methanogens that use H_2 as a primary energy and electron source to achieve CO_2 conversion in a non-reversible and selective way. While combining solar H_2 production with biomethanation poses additional challenge in terms of process integration and safety, this would allow a significant reduction in the carbon impact of green methane production units, with a minimal energy cost. Here we present the autonomous solar integrated fuel (EASI Fuel) device, based on integrated photoelectrochemical (IPEC) cells with a total light-harvesting surface of 342 cm² producing solar hydrogen to feed a frugal bioreactor where green methane is produced from CO_2 by methanogens. The

EASI Fuel device was one of the three finalists of the European Innovation Council challenge "Horizon Prize - Fuel from the sun: Artificial Photosynthesis" which acknowledged its originality and high standard of integration[a]. We discuss its design in terms of integration and future scaling as well as measured performance during long-term runs under natural solar irradiation, hence demonstrating achievement of a Technology Readiness Level (TRL) of 5.

Results and Discussion

A compact and integrated design for intensification and scalabilty

The principle of the EASI Fuel device for solar methane production is depicted in Figure 1. The originality of the developed system lies in the interfacing of a solar water splitting system, self-sufficient for hydrogen production from water under sunlight, with a methanogenic bioreactor for methane formation from CO_2 (Equation 1) in a continuous way and near ambient pressure and temperature.

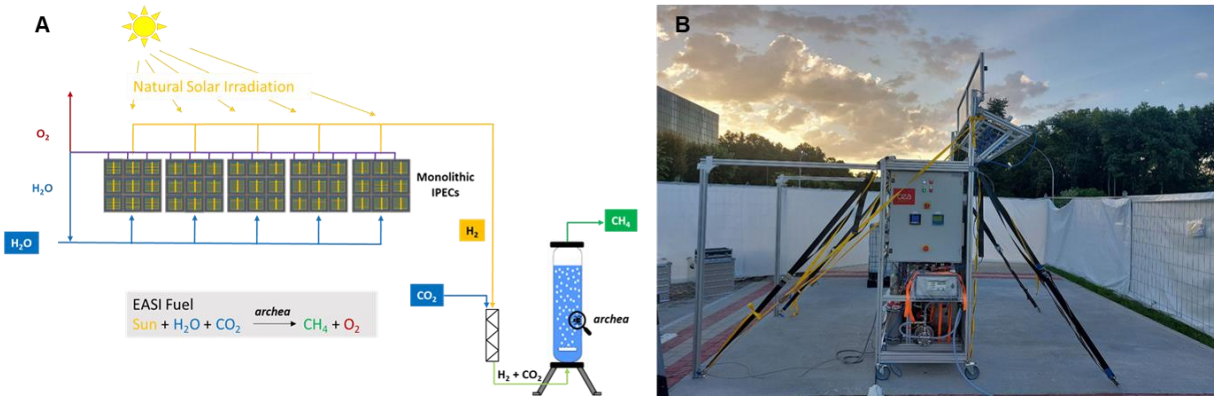

Figure 1. [The EASI Fuel device installed at JRC Ispra]
(A) Schematic view of the EASI Fuel device with IPEC modules in series and bioreactor.
(B) Picture of the EASI Fuel device installed for a 3-day demonstration test at the JRC in Ispra in July 2022.

Integrated Photoelectrochemical Cells.

Solar hydrogen is produced by a series of 45 IPEC cells (6.5 × 6.5 cm^2) assembled in 5 monolithic modules (21 × 22 cm^2).

Each IPEC cell consists in the association of a silicon / perovskite (Si/PK) tandem solar cell and a hybrid polymer-metal proton exchange membrane (PEM) electrolyser (Figure 2). The 9.0 cm^2 Si/PK solar cell (n-i-p architecture)[20] with a solar active area of 7.6 cm^2 ensures photons collection in the 300-1200 nm range thanks to a perovskite top-cell (optical band gap 1.58 eV, UV-visible absorption until 750 nm) deposited onto a silicon heterojunction bottom-cell (optical band gap 1.12 eV, UV-visible-near IR absorption until 1200 nm) and connected in series through an ITO (Indium Tin Oxide) recombination layer. As depicted in Figure 2, the voltage addition of both sub-cells reaches 1.35 - 1.45 V at the maximum power point under 1 sun enabling overall water

[a] European Commission, Directorate-General for Research and Innovation, Fuel from the sun : Artificial Photosynthesis – EIC Horizon Prize – Commissariat à l'énergie atomique et aux énergies alternatives (CEA), Publications Office of the European Union, 2022, https://data.europa.eu/doi/10.2777/18380

splitting in a PEM electrolyser based on a typical Ir black/Nafion NRE-112/Pt-C membrane electrode assembly (MEA) prepared by hot pressing. A Au-coated 3D-printed polypropylene flow-plate, as described previouly by Cronin and coworkers[21] and a platinized titanium grid as current collector were used at the anode side. At the cathode side, a 3D-printed metallic flow plate in stainless steel (316 L type), with built-in pin flow channels,[22] also acts as both current collector and electrical contact for the Si/PK tandem solar cell.

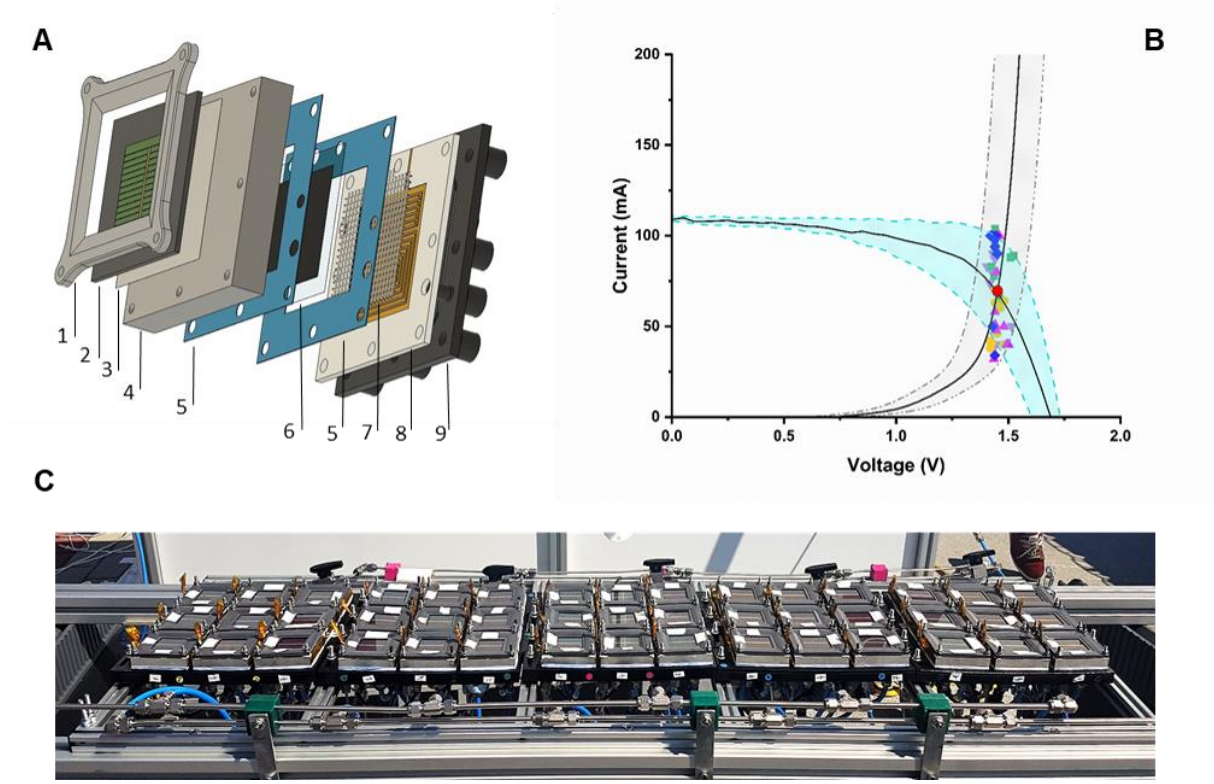

Figure 2. [The Integrated Photoelectrochemical Cells and modules]
(A) Exploded view of an IPEC cell: 1. mask, 2. Si/PK solar cell, 3. indium sheet, 4. 3D-printed cathodic flow plate with integrated heat exchanger, 5. silicone gasket, 6. membrane-electrode assembly, 7. platinized Ti grid, 8. gold-coated anodic flow plate, 9. plastic support.
(B) The solid black lines corresponds to the I-V curves of the components of a typical IPEC cell (Si/PK tandem solar cell of 7.6 cm^2 active area, and corresponding PEM electrolyser) whose intersection materializes the operating point (filled red dot). The filled colored symbols (■◆▲▼●) represents the actual operating points of the 45 IPEC cells, measured before the 72 h outdoor test at the JRC, in Ispra, in July 2022. Each colored symbol corresponds to one of the 5 IPEC modules; the shaded blue and grey area represent the dispersion of I-V curves for solar and PEM cells, respectively.
(C) Picture of the 5 monolithic modules installed on the EASI Fuel device.

Additionaly, a heat exchanger was integrated in the bulk of the cathodic flow plate, in order to exploit heat generated at the solar cell to raise the water temperature to approx. 50°C, at a typical flow rate between 1 and 5 $L.h^{-1}$, before it is delivered at the anode side, as described in detail elsewhere.[12] In each monolithic module comprising 9 IPEC cells (total solar active area of 68.4 cm^2, Figure 2), the fluid management was designed both to connect the 9 heat exchangers in series, hence maximizing the water temperature, and to evenly distribute the pre-heated water flux to 3 series of 3 IPEC cells.

This design allows to limit the holdup of O_2 bubbles and electrical resistance created by such bubbles in the anodic compartment.[23]

Wireless electrical integration of the Si/PK solar cell was ensured with a 100 µm-thick indium sheet between its rear electrode and the cathodic flow plate of the electrolyser, enabling the direct use of the photogenerated electrons at the cathode. Positive charges delivered by the PK top cell are transferred to the anode of the electrolyser via a Pt wire. The cell fixation on the cathodic plate has been strengthened with a plastic 3D-printed mask that precisely defines the illuminated surface of the solar tandem cell (9.0 cm^2). The 9 IPEC cells in each module are therefore electrically independent, so that the failure of one solar cell or PEM electrolyser, or shading effects likely to occur outdoor, do not affect the performance of the others.

The operating point of each IPEC cell lies at the crossing between the I-V curve of its Si/PK cell and that of the PEM electrolyser. Figure 2 shows the distribution of the operating points of the 45 IPEC cells assembled in the 5 modules used in the EASI Fuel device, as measured prior to long term testing at Ispra. All operating points lie close to 1.45 V. The variation in photocurrent is due to the exponential shape of the I-V curves in this voltage range (see Figure 6).

Strain selection and bioreactor.

The anaerobic methane-producing *Methanococcus maripaludis* has been selected for its easy and fast growth under H_2/CO_2 feed, at ambient temperature (20-40°C).[24] A specific bubble column bioreactor (BCR) was designed and realized[25] to implement the conversion of solar H_2 and CO_2 into green methane (Figure S6). Its innovative, frugal, robust and modular architecture meets both the need for maximizing the bioavailability of the gas to the microorganisms,[26] and for notably reducing the energy consumption, as compared *e.g.* to the direct upscaling of lab-scale mechanically stirred bioreactor (Continous Stirred-Tank Reactor or CSTR)[27]. Beyond the significant increase of H_2 residence time and gas-liquid exchange surface, provided by dispersing the gas in the form of small bubbles in the culture medium, the biological conversion of the H_2/CO_2 mixture into CH_4 is further optimized by recycling the outlet gas flux at the bottom of the reactor, where it is redispersed as bubbles, thanks to a porous metal diffuser and a high recirculation flow of 10 $L.h^{-1}$.

The reactor was tested for long periods of times, and its sensitivity to various parameters, including temperature, inlet pressure, inlet gas flow, and of course intermittent supply of H_2/CO_2 mixture to simulate day-night cycles, was evaluated with bottle gas supply. The achieved selectivity and efficiency of CO_2 conversion into CH_4 determined by chromatographic analysis were remarkable with an output gas mainly composed of methane (volume fraction X_{CH4} of 87 vol%) and no side product other than H_2 (X_{H2} = 11 vol%) and CO_2 (X_{CO2} < 2 vol%) under operational conditions (P = 2 bar, T = 37°C, X_{O2} = 0 vol%). The strain exhibited stable performances for over one month without addition of fresh growth medium. The detrimental effect of O_2 on these oxygen-sensitive microorganisms was prevented by the use of an O_2-scavenger system, ensuring a maximum O_2 concentration below 0.05% in the H_2 flow along the experiment.

System Integration: from light capture to fuel production

The autonomous device combines the electrical, thermal and fluidic integration of the 5 IPEC modules (Figure 2, 45 IPEC cells in total) with the bioreactor, together with an automation system allowing for autonomous operation and for the collection of process

monitoring relevant data. The process and instrumentation diagram (PID) of the device is provided in Figure 4. Autonomy of the system is ensured by an OPTO 22 type PLC with several analog and digital input/output modules.

A specific and in house control and command program was developed under the Pack Display Basic© software suite. Its operation is structured around the programming of 4 control loops (for the regulation of the IPEC modules water flow, the overpressure of the H_2 produced, the composition of the H_2/CO_2 inlet mixture, and the pressure within the bioreactor, respectively), followed by 5 safety actions (concerning the O_2 content in the gas mixture fed to reactor, the IPECs pressure, the default of water supply to the modules, the bioreactor pressure and the temperature of the O_2 traps, respectively) and 2 nominal "day" and "night" operation modes to adjust the electrical consumption to the intermittent H_2 production.

Deionized water is supplied continuously to the IPEC modules from a 300 L tank (Figure 3, left) by a flow controlled pump. The on-line removal of possible oxygen trace in the solar hydrogen, before being mixed with CO_2, to avoid the risk of O_2 contamination in the reactor, was the main challenge encountered to couple solar H_2 production and biomethanation. The water content in the output gas of the IPEC modules must also be limited because of the sensors sensitivity to humidity. Two catalytic filters (activated copper oxide and aluminum oxide for O_2 removal and zeolites for dehumification) in parallel are used in this aim[b]. The oxygen content is then measured and a third catalytic filter is placed to remove any residual O_2 in the H_2 gas. Once purified, H_2 accumulates upstream from an adjustable pressure valve, until it reaches a sufficient pressure (down to 20 mbar) and is then mixed in real time with CO_2. The mixing plate consists of a pressure reducer, a flow controller and a static mixer. The gas composition is adjusted to the stoichiometry required for the reaction (Equation 1), *e.g.* 80 vol% H_2 – 20 vol% CO_2. The mixture is then transferred, by a volumetric pump, to the bioreactor at a pressure slightly higher than the one prevailing inside the bubble column, therefore avoiding the need for a compressor.

As the bioreactor nominally operates between 25°C and 35°C, no additional heating was found necessary in the summer period. A reversible Peltier thermoelectric module was however included in the device to maintain the temperature between 25°C and 40 °C if needed. The continuous conversion of solar H_2 and CO_2 into CH_4 and H_2O causes the pressure in the reactor to change, especially as the 3 gases have different solubilities in the aqueous culture medium. Consequently, a constant pressure of 1.5 bar is maintained in the bioreactor by means of a pressure gauge located in the headspace. For the 2 L liquid column used in the demonstrator, and at the chosen operating pressure and temperature (1.5 bar, 35°C), the maximum gas retention in the reactor is 0.72 L. The outlet gas is dehumidified with zeolites filters, then volumetrically quantified and analysed using infrared sensors in order to determine the CH_4 and CO_2 fractions. Finally, it is stored in a flexible tank (Musthane®) made from rubber-coated fabric, with a maximum volume of 10 L and admissible pressure of 2 bar.

Designed at TRL 5, the EASI Fuel device is autonomous, occupies about 2 m^2 and is able to steadily deliver 12 $Wh.day^{-1}$ of methane fuel in a summer day. The device was subjected to ATEX certification by an approved body (APAVE) before its installation and commissioning in Ispra. Only the auxiliary elements, such as pumps, flow-

[b] In the version of the prototype used in Grenoble for the autumn testing campaign, an additionnal gas-liquid separator was added prior two O_2/H_2O filters.

regulators, sensors, whose consumption has been minimized (and could be mutualized at larger scale), used the electrical network.

Figure 3. [Details of the EASI Fuel device]
(A) Side view showing the bioreactor in the front (see Figure S6 for an enlargement) and the feed water tank in the back.
(B) Back view showing the control panel.
(C) Side view showing 4 of the 5 IPEC modules for solar H_2 production.

Real-life tests to assess the device versatility and resilience

The device autonomously operated outdoor for two periods of 72 hours each. The first trial period took place on July 4-7 during summer 2022 in Ispra (Italy), within the framework of the EIC Challenge « Fuel from the Sun: Artificial Photosynthesis » grand finale, while the second test was performed on October 4-7 in autumn 2022 in Grenoble (France). Detailed results and the overall performance achieved during these two demonstrations in real conditions are shown in Figure 5 and S1 and discussed below.

Figure 5 presents the time-evolution of the green fuel (CH_4 + H_2) production during the summer test in Ispra, along with the corresponding transient global horizontal irradiance, which was recorded from the ESTI Meteo Tower. Additional graphs depicting the production of solar H_2 in Ispra (Figure S3), as well as the time-evolutions of green fuel (Figure S1) are given in the supplementary information section.

During the summer measurement campaign, the actual duration of methane production was limited to 18 h 15 min, mainly due to the weather conditions (in particular, we had to force the system to shut down due to heavy rain in the first day, to protect the Si/PK tandem solar cells), and due to the malfunction of the dehumidification system impeding the oxygen sensor and related triggering of the safety system installed on the device. As a result, the time required to reach a nominal state of the entire system was relatively long compared with the duration of the test campaign, with the onset of H_2 production observed after 4 h 14 min of operation. This time was taken as the starting point for determining the system performance (Table 1 and Figure 5). The 2nd and the 3rd days exhibited a more regular trend, with similar average values for both global normal irradiance (800 W.m^{-2}) and global horizontal irradiance (500 W.m^{-2}). On the 3rd day, the pressure threshold of the solenoid valve, responsible for directing hydrogen flow into the reactor, was reduced from 50 mbar to 20 mbar to compensate for the aging of the tandem solar cells. The system continued

to operate remarkably well with such a low overpressure. During this first testing campaign, the device demonstrated its capacity to adapt to a wide range of operating conditions, including the alternative day-night H_2 gas supply, and to stop and restart according to the weather conditions, thanks to the remarkable stability of the Archaea culture.

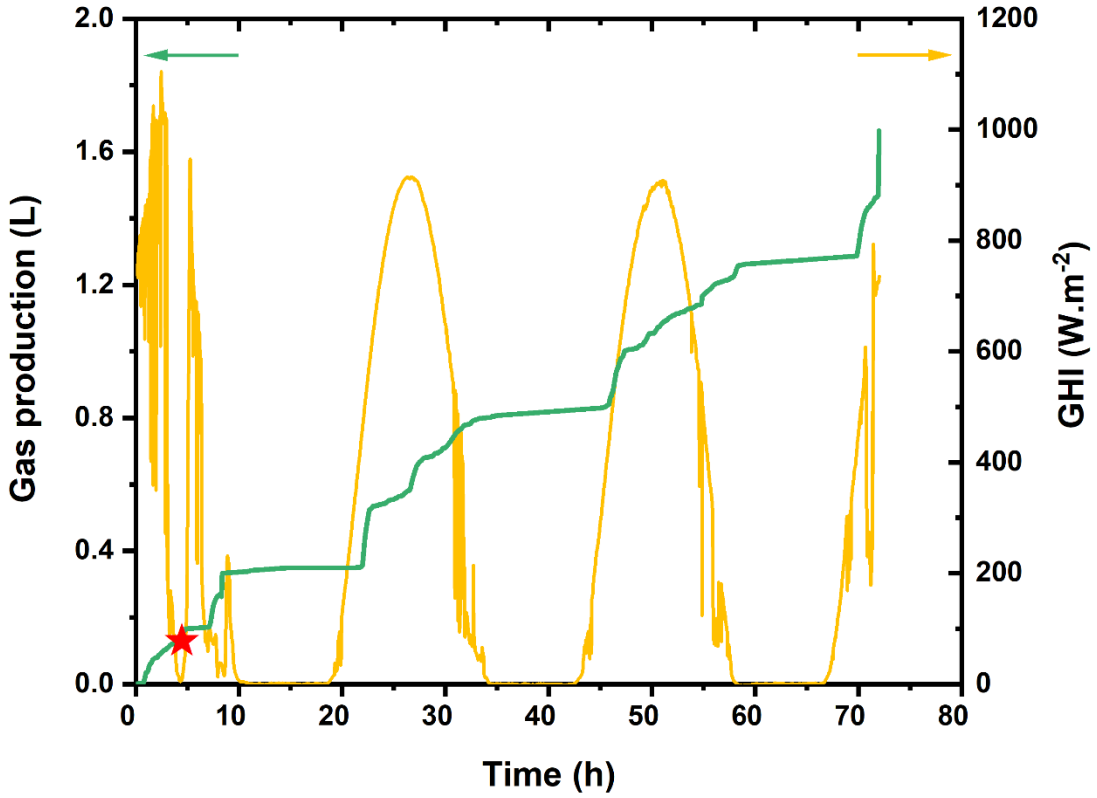

Figure 5. [Performance of the EASI Fuel device during outoor test in Ispra]
Cumulated volume of gas produced in green; Global Horizontal Irradiance (GHI), in yellow. The red symbol materializes the beginning of the measurement campaign.

The test in Grenoble (Figure S1) was achieved with aged *(i.e.* degraded) Si/PK tandem solar cells and after their decoupling from all IPEC cells, individual testing (see Figure 6) and reassembly of 36 IPEC cells with the best performing Si/PK tandem solar cells. It had a total duration of methane production of 28 h 20 min. During this second campaign, in addition to the continuous monitoring with a non-dispersive infrared (NDIR) sensor, we could determine the composition of the gas leaving the bioreactor by gas chromatography. Both measurements proved consistent, indicating a fuel composition of X_{CH4} = 89 vol% and X_{H2} = 11 vol%, similar to that considered to determine the methane production rates and solar-to-fuel yields in Ispra (Table 1) and in Grenoble. During this second campaign, the temperature could also be monitored at different places of the EASI Fuel device (Figure S2).

Table 1. [System specifications and achieved performance at the JRC in Ispra in July 2022]

The reported data were calculated by subtracting the gas volume already present in the reactor (0.14 L) at the beginning of the measurement campaign. Total incident solar energy E_{GHI} and solar-to-hydrogen yield STH_{GHI} are based on the values of Global Horizontal Irradiance (GHI, direct and diffuse incident irradiance measured on a horizontal plane); the same applies for the solar-to-fuel yield STF_{CHI}. The $[Photon\ Flux^{3rd\ day}]_{1\ sun}$ and the Quantum Efficiency $\left[QE_{Fuel}^{3rd\ day}\right]_{1\ sun}$ are calculated for the 3rd day of production when the irradiance was closer to 1 sun during the operating hours.

	JRC in Ispra			
Date (2022)	July 4	July 5	July 6	July 7
Number of IPEC modules	5			
Total test / prodution time (h)	72 / 18.25			
Daily production time (h)	2.22	7.29	8.17	0.57
Average GHI ($W.m^{-2}$)	105	557	437	716
Max GHI ($W.m^{-2}$)	969	914	909	793
E_{GHI} ($Wh.m^{-2}$)	237	4082	3600	442
STH_{GHI} (%)	17.13*	6.53	7.42	2.46**
Average H_2 production per hour of operation ($L.h^{-1}$)	0.37			
r_{H_2} ($mol.m^{-2}.h^{-1}$)	0.49			
Weighted average of STH_{GHI} (%)	7.00			
Average CH_4 production per hour of operation ($L.h^{-1}$)	0.075			
$[Photon\ Flux^{3rd\ day}]_{1\ sun}$ ($mol.m^{-2}$)	69.40			
$\left[QE_{Fuel}^{3rd\ day}\right]_{1\ sun}$ (%)	4.54			
r_{Fuel} ($mol.m^{-2}.h^{-1}$)	0.11			
STF_{GHI} (%)	5.48			
Average concentration of O_2 in the H_2 flow during operating time (%)	0.049	0.022	0.028	0.021
Max O_2 detected in the H_2 flow during the day (%)	> 1 %	> 1 %	0.055	0.034
Reactor Pressure (bar abs)	1.20	1.41	1.40	1.34
Average H_2 Pressure (bar abs)	0.969	0.995	0.988	0.975
Max H_2 Pressure (bar abs)	1.433	1.558	1.554	1.411
Max instantaneous power consumed (W)	132	132	134	133

* This high STH value on July 4th, although consistent with preliminary results obtained from laboratory tests on “fresh” IPECs (unpublished results), has not been included in the average yield, due to uncertainties related to the actual production time.

** Similarly, the data for July 7th were not included in the calculation of the weighted average STH, due to the short duration time and instability of the system during the first 30 minutes of the early morning operation.

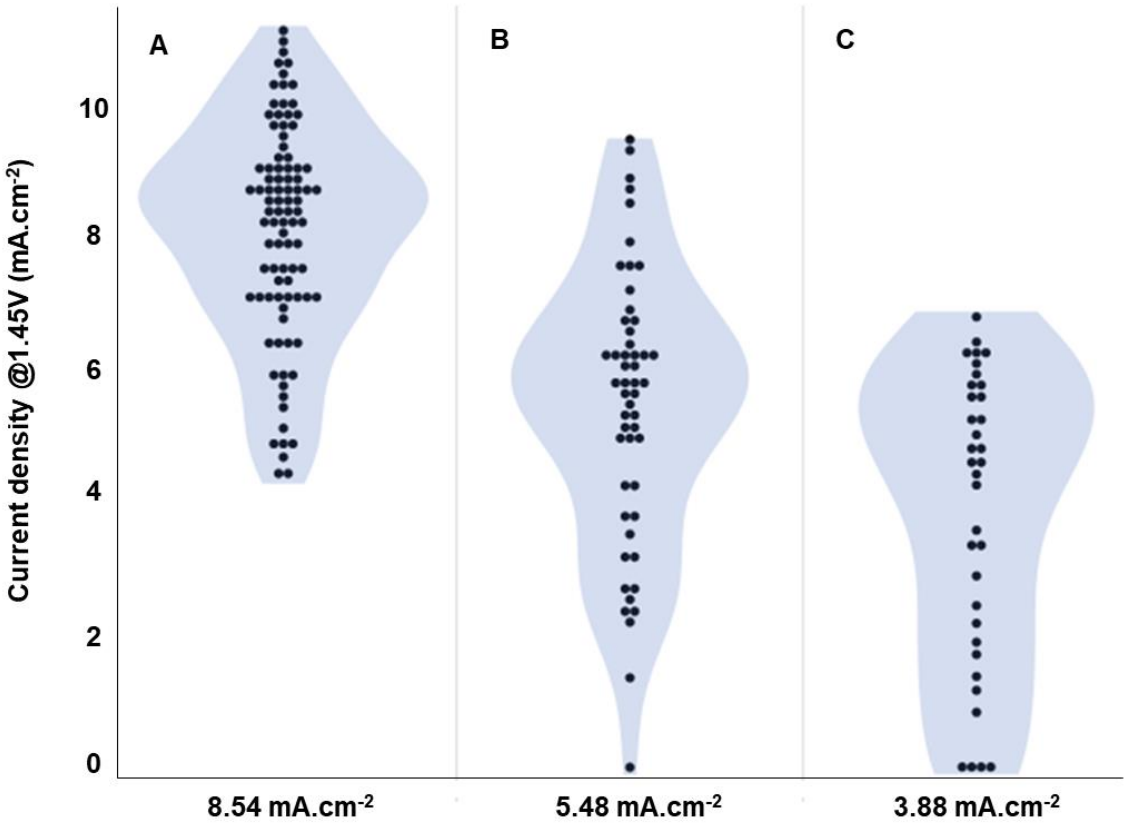

Figure 6. [Impact of the degradation of the solar cells]
Evolution of current density produced under 1 sun at 1.45 V (close to IPEC cells operating point) by the 45 tandem Si/PK solar cells integrated into the EASI Fuel device. For the measurements, the solar cells were decoupled from the electrolysers. Average current density values are indicated on the bottom of each dataset.
(A) Initial performance (before integration).
(B) After the 1st outdoor test.
(C) After the 2nd outdoor test.

Discussion on device performance

Solar-to-Hydrogen and Solar-to-Fuel yield

During the first test campaign, the 5 monolithic IPEC modules, with a total capture area of 342 cm², produced hydrogen at a rate of 0.37 $L.h^{-1}$. This corresponds to an average STH_{GHI} of 7.0 %, over 72 h of continuous outdoor testing, with 18 h 15 min of solar irradiation. To the best of our knowledge, this is one of the very few examples[28,29] of devices producing solar hydrogen tested under such real life conditions. The STH performance measured under such conditions ranks well with the current state of the art for similar integrated solar-to hydrogen devices[13,29–31] working under non-concentrated solar conditions. Importantly, outdoor-measured STH values of fixed-array devices are expected to be lower than those determined in lab conditions since the outdoor irradiance is lower at sunrise and sunset. In addition, the area of the solar cells used here is significantly larger than most integrated devices reported so far which show better performance (typically below 1 cm²)[17,31].

This average value actually captures the significant degradation of the tandem Si/PK solar cells (see below) with a significantly higher STH_{GHI} achieved in day 1 (~17 %) compared to the subsequent days (~ 7% on day 2 and 3, ~2.5% on day 4) as reported in Table 1.

The total volume of hydrogen produced by the IPEC cells (approximately 7 L over the 72 consecutive hours of the first testing campaign) was gradually converted into a green fuel primarily consisting of CH_4 and unreacted solar H_2, by reaction with bottled CO_2 in the bioreactor. The solar-to-fuel yield was calculated at 5.5% over the 72 hours of testing, a value that stands out among other reported systems for converting CO_2 into hydrocarbons[32–40].While systems producing formic acid, CO or syngas have been reported with higher STF efficiencies, they were of small size, not tested outdoor and not optimized toward a high conversion of CO_2. The EASI fuel device also ranks well in performance compared to solar photothermal CO_2 conversion into syngas.[41]
The tests performed in Grenoble showed results consistent with the progressive degradation of Si/PK tandem with a solar-to-fuel yield of 2.7 %. Meanwhile, the average CH_4 production per hour of operation was 0.04 $L.h^{-1}$, and the fuel product rate was 0.06 $mol.m^{-2}.h^{-1}$. This performance was achieved under an average GHI of 537 $W.m^{-2}$ (typical sunshine in autumn in this region), a cumulative E_{GHI} of 14246 $Wh.m^{-2}$, for a total operating time greater than in Ispra but with a reduced number of IPEC modules (36 IPEC cells corresponding to 4 IPEC modules) equipped with aged solar cells. Finally there is a proportional relationship between the two measurement campaigns.

Solar cells degradation: a major bottleneck that limits green methane production

While the sequence of tests had no impact on the conversion of CO_2 into methane, which performed remarkably well for months,[25] the performance of the IPEC cell continuously decreased during the testing periods, which was attributed to the degradation of the solar cells (as already observed for other types of IPEC[42]).
The impact of this degradation is particularly visible in Figure 6.
These graphs present the evolution of the current density produced by the tandem Si/PK cells at 1.45 V and measured under calibrated 1 sun conditions, before integration in the IPEC cells, and after each outdoor testing campaign (for these measurements, the solar cells were dismounted from the IPEC cells). The operating current density decay observed after ageing is consistent with and explains the decrease in STH measured over time (Table 1). Actually, the I-V curves of the solar cells recorded after outdoor ageing (Figure S4) show significant fill factor (FF) losses.
Interestingly, these losses seem correlated to the position of the Si/PK tandem solar cells in the IPEC modules (see Figure S5 and Table S1): losses are minimized (18 %) for Si/PK tandem solar cells placed close to the water inlet, while solar cells at the end of the heat exchanger suffer from major degradations (up to 65 %), suggesting that among stress factors, not only illumination but also heat might play a major role in outdoor ageing.

Market potential

While the EASI Fuel device exploits bottled CO_2 gas, the deploiement of solar fuel technologies will require the coupling of the conversion units to either point source supply or air capture plants. Methanogenesis is considered as a promising route for biogas upgrading[43]. Electrochaea project investigates biomethane production with H_2 produced electrochemically, targeting a 10 MW device based on thermophilic strains

of Archea, which beneficiated from EU fundings in 2020[c]. Accordingly, we found that the best market opportunity for the EASI Fuel technology would be to couple solar methane production to a methanisation unit, in order to benefit both from its large biosourced CO_2 output, with specification already compatible with the biological methanation process in the device, and from the existing operational connexion of such biogas plants to the natural gas distribution network.

A preliminary economic assessment was carried out in 2021. It was based on the coupling of the EASI Fuel system with a 2MW methane production unit providing a continuous flow of around 200 Nm^3/h of CO_2 without significant seasonal variations, such as the Biometharn facility in the South of France[d], to provide an average production of approx. 100 m^3/h of additional CH_4 thanks to the solar device. The estimated production cost of this green CH_4 was 3.5 times higher than the purchase price of biomethane in France over the same period, with the PEC and bioreactor making an equivalent contribution to this cost. The study also highlighted that coupling the EASI Fuel system with an intermediate H_2 storage, to delay one half of the daily production at night, could reduce the price by up to 40%, thanks to the induced reduction in bioreactor investment and exploitation costs.[e] In addition, the thermal coupling of the EASI Fuel bioreactor with the biomethaniser will ease managing heat variations in the two devices, both of which needing to operate at similar temperature with intermittent energy sources.

In France, the deployment of methanisation is still in progress. The AFG (Association France Gaz) expects a global market of 50 TWh for biogas injected in the French natural gas network by 2030.[f] Taking into account the constraints for the minimal size of the biomethaniser unit (at least 1 MW) and the land constraint for techno-economic viability (a few hectares available), a good estimate of the minimum potential in the French context is around 10% of the global offer, hence around 5 TWh for France, and the valorisation of 500,000 m^3 (820 tons) of CO_2 per year. In Italy, where biogas is more developed but where most units are dedicated to electricity production[44], there is an opportunity to convert some of these units to biomethane production. By transforming some of the co-produced CO_2 to methane thanks to solar hydrogen, the EASI Fuel device will extend the biomethane capacity of the converted plant, obviously increasing the opportunity to convert the current electricy dedicated biogas plant to a biomethane plant.

Conclusion and perspectives

The EASI Fuel device demonstrates solar methane production at a technological readiness level (TRL) of 5 according to the EU definition[g]. It relies on solar H_2 production in IPEC cells where thermal and fluidic integration allowed to intensify both performance and stability compared to classical PV + EC systems via a limitation of the solar cells heating (which affects their efficiency and lifespan)[45] and the preheating of water which lowers the voltage of the electrolysis cells. The proper selection and

[c] Electrochaea project. http://www.electrochaea.com/technology/

[d] www.biometharn.fr

[e] The results of this evaluation are detailed in the EIC challenge application file, which can be made available on request. Assumptions were based on 2022 prices, which are no longer relevant since the war in Ukraine and the global energy context.

[f] https://www.francegaz.fr/wp-content/uploads/CP-LAFG-devient-France-gaz-1.pdf

[g] https://ec.europa.eu/research/participants/data/ref/h2020/wp/2014_2015/annexes/h2020-wp1415-annex-g-trl_en.pdf

adaptation of a mesophilic methanogen strain and its growth medium to near ambient temperature and at moderate pressure, coupled with the inventive design of a frugal bioreactor were the key to the direct chaining of solar H_2 production. Such a biological system provides significant flexibility for the direct conversion of solar hydrogen into methane and the EASI Fuel device opens up the possibility of producing high-purity methane in environments where access to electricity is limited. The current demonstration has been made with solar cells that, though not at the state of the art regarding their performance and stability, bear the promise for greater STH, STF and device lifetime. To improve device performance and stability, we therefore need both to improve the shape of the Si/PK tandem solar cells characteristic curve to maximize operating voltage, which we have begun to do by modifying the thickness and composition of the perovskite and p layers of the perovskite sub-cell[12] and to optimize the encapsulation process[46]. Progress brought by the community regarding perovskite/silicon tandem solar cells have steadily been reported, with recent power conversion efficiencies of 32.5,[47] 33.7[h] and 33.9[i] %, now surpassing the theoretical limit for single junctions. Long lasting performance has also been demonstrated, for example in studies with year-long outdoor operational lifetimes.[45]

Future optimisations regarding the development of noble metal-free catalysts and use of fluorine-free membranes will also further lower the environmental impact and increase the economical viability of this technology. In the short term, the use of stable, cheap but less efficient single-junction absorbers such as silicon, although not economically attractive,[48] could be a relevant option to demonstrate the scalable and reliable coupling of direct solar hydrogen generation and methanogenesis. Furthermore, additive manufacturing technologies should in the future allow to increase the degree of integration of this hybrid solar fuel generator by extending the concept of monoblock geometry, here limited to the PEM module, to the overall device. This will enable to further reduce the weight of the structure, minimize the need for materials and connectors, and increase its compactness, hence paving the way for new industrial and domestic applications of solar fuels.

Experimental procedures

Resource availability

Lead contact:

Further information and request for resources should be directed to Sophie Charton, sophie.charton@cea.fr.

Materials availability:

This study did not generate new unique materials.

Data and code availability:

The main data supporting the findings of this study are available within the paper and its supporting documentation.

Monitoring of gas production and safety limits

[h] https://www.pv-magazine.com/2023/05/30/kaust-claims-33-7-efficiency-for-perovskite-silicon-tandem-solar-cell/

[i] https://www.pv-magazine.com/2023/11/03/longi-claims-33-9-efficiency-for-perovskite-silicon-tandem-solar-cell/

O_2 monitoring and safety. At the outlet of the IPEC modules and before the mixing operation with CO_2, the device is equipped with a compact oxygen transmitter that uses proven sensor technology (oxy.IQ2 oxygen sensor) to measure the volume fraction of O_2 in the gas produced by the IPEC. More in detail, the oxygen sensor is an advanced galvanic fuel cell (0 - 1000 ppm); the transmitter is installed after two O_2/H_2O reducing filters (CRS - 202295-5S) in parallel, which, under normal operating conditions, allow to reach O_2 content of less than 5 ppb, and H_2O content of less than 20 ppb. The measurement of the O_2 concentration is monitored to enable system shutdown in case of a filters failure, which would compromise process integrity.

To ensure the device security, two safety thresholds have been programmed in the O_2 sensor. The first threshold corresponds to 1% of the lower explosive limit (LEL) of hydrogen in air, and is the threshold above which the device may present a risk to humans. If this threshold is exceeded, all hydrogen production is evacuated from the demonstrator, and a purge with neutral gas (argon) is performed throughout the hydrogen production area to evacuate any contaminated gas from the demonstrator. The second threshold, set at a concentration of 0.1 vol% O_2 in H_2, corresponds to the point at which the process is at risk. At this threshold, the biological system can be severely degraded, adversely affecting methane production. When this threshold is exceeded, hydrogen production is directed away from the device so as not to introduce oxygen into the biological part of the demonstrator. Moreover, to prevent any risk of deterioration of the biological part, a third O_2/H_2O filter (CRS - 202295-5S) is positioned downstream of the O_2 sensor to ensure maximum reduction of the oxygen content (O_2 < 0.1 vol%). Finally, initial experiments carried out on the device showed that the moisture contained in the gas, coming from the IPEC modules, tended to condense before passing through the filters, greatly reducing filtration efficiency. For the autumn testing campaign, the device was therefore fitted with a liquid gas separator upstream of the filtration system to capture any source of liquid water. As an additional safety measure, and to avoid the accumulation of the oxygen produced by the IPEC modules, a potential source of explosion, the water leaving the electrolyser was collected in an open air recovery tank ("R163" tank in Figure 4).

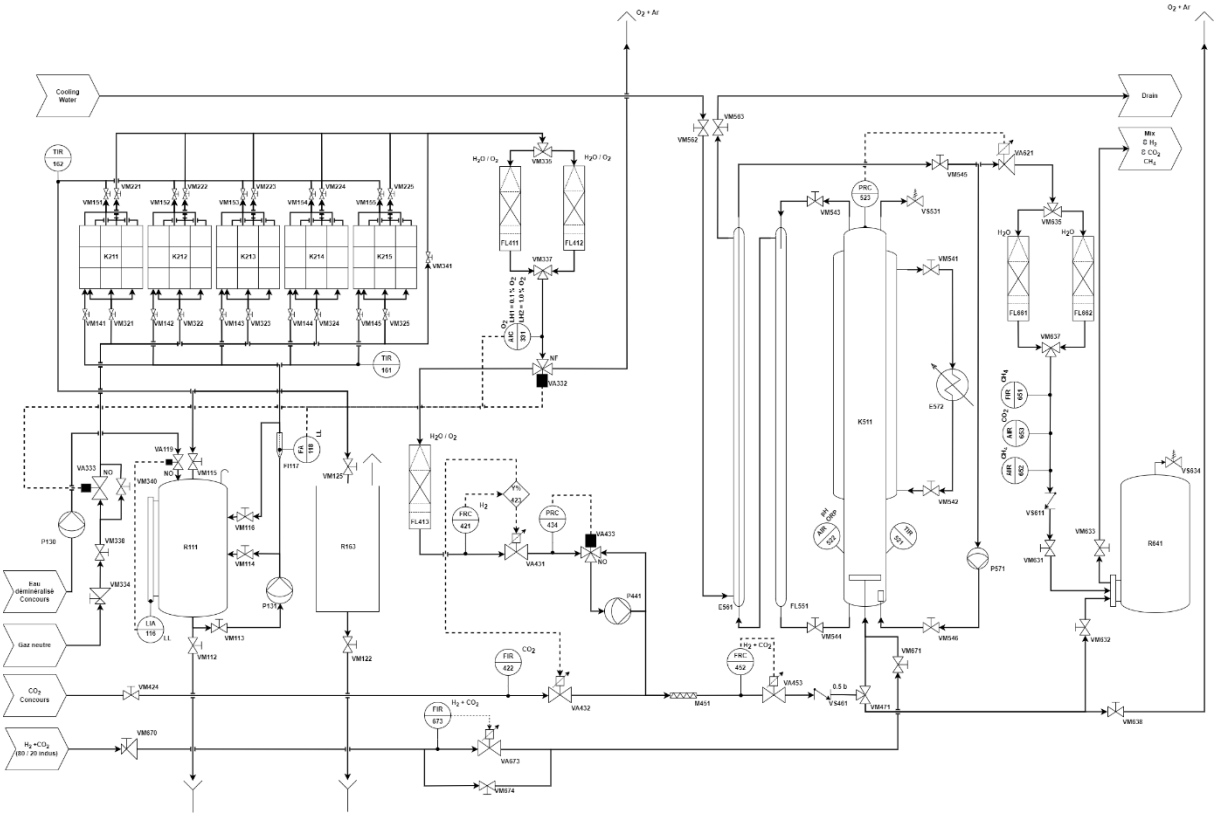

Figure 4. [Process and instrumentation diagram of the EASI Fuel device]
See Table S2 for the nomenclature.

Produced gas control and supply. In addition to sensors dedicated to safety, the system is equipped with various sensors required for monitoring and data acquisition. All gas flows are measured using BROOKS SLA5850S thermal mass flowmeters, with the exception of the gas flow produced at the reactor outlet, which is measured using Bronkhorst EL-FLOW F-201CV thermal mass flowmeters. Pressure is measured using KELLER serie 23 absolute pressure transmitters. The residual CH_4 and CO_2 composition in the gas produced is obtained by infrared measurement (NDIR) using 2 smartGas FLOW evo sensors (CH_4 sensor : F3-043108-05000 and CO_2 sensor : F3-214507-05000), respectively calibrated over a range of 0 to 100%vol and 0 to 50vol%. The bioreactor chamber is also equipped with measuring instruments to monitor the condition of the biological system. The bioreactor is equipped with a Mettler Toledo INPRO3253i probe for simultaneous measurement of pH, redox potential and temperature of the culture medium. The thermal sensors for mass flow and gas composition measurement (NDIR) are sensitive to the humidity that may be contained in the gas. To protect this equipment, moisture traps (CRS - 202230-SS) are installed at the outlet of the bioreactor outlet. Finally, all signals measured on the device are transmitted to the programmable controller for recording or use in plant automation.

For information, all bottle of gas used to test the device were supplied by the gas manufacturer "Air Products" with a certified purity level > 99.999%. For verification and calibration of the CO_2 infrared sensor, the gas used was a mixture of CO_2 and N_2 in equivalent proportions (50/50 vol%). For calibrating the CH_4 infrared sensor, the gas used was pure methane. The device is also equipped with an argon-based inert gas cylinder and an 80/20 vol% H_2 - CO_2 gas mixture, used to maintain biological cultures between experiments.

Irradiance monitoring

In Ispra, the values of Global Horizontal Irradiance (GHI) were recorded from the ESTI Meteo Tower (J.R.C. Ispra || 45° 48' 43.4' N - 8° 37' 37.4' E || altitude: 220 m), positioned approximately 100 m from the EASI Fuel Device. Incident power in the IPEC plane was not recorded. Solar to fuel efficiencies are calculated against GHI and are therefore likely to be overestimated by maximum 10 % (Figure S7), as horizontal irradiance is lower than normal irradiance. To keep the reader aware of that, STH and STF are explicitly denoted with a GHI subscript.

The photon flux was registered with a In-Plane spectroradiometer mounted on the EKO Sun Tracker STR-32G, that followed an azimuth-elevation algorithm and was therfore not in a fixed configuration like the IPEC modules. Consequently, the $\left[QE_{Fuel}^{3rd\ day}\right]_{1\ sun}$ for the fixed array of IPEC modules is likely to be underestimated, depending on the photon flux.

On the other hand, in Grenoble, the Global Horizontal Irradiance was measured by a static Kipp & Zonen CMP10 pyranometer.
Thus, the comparison between the two test campains can be made by considering the results depending on the Global Horizontal Irradiance (Table 1, Figure S1), calculated during both the summer and autumn campaigns.

Data analysis and performance calculation

All calculations have been carried out considering standard conditions of pressure and temperature (earlier IUPAC definition, 0 °C and 1.013 bar).

The solar to hydrogen efficiency[2] is calculated according to the following Equation:

$$STH = \frac{Output\ energy\ as\ H_2}{Energy\ of\ incident\ solar\ light} = \frac{n_{H2}\ (mol) \times \Delta G_r\ (J.mol^{-1})}{E_{sun}\ (Ws.cm^{-2}) \times A\ (cm^2)}$$

n_{H_2} is the amount (in mole) of Hydrogen, ΔG_r is the reaction's Gibbs free energy (237 $kJ.mol^{-1}$) for water splitting reaction at 298 K, corresponding to 1.23 V, that is the thermodynamic water splitting voltage. E_{sun} is the total incident solar energy ($Ws\ cm^{-2}$) and A is the irradiated active surface (cm^2).
The product rate (i.e. quantity of product)[49] per irradiated active surface (A) and time (h of production) can be expressed by :

$$r_{product} = \frac{n_{product}\ (mol)}{A\ (m^2) \times t(h)}$$

This equation is used to calculate both the H_2 produced from electrochemical water splitting, and the fuel produced during the production hours.

Volume of produced fuel inside the reactor. The effective production of hydrogen in Ispra started at t_0+ 4 h 14 min (1:14 pm). Consequently, all the methane produced before 1:14 pm was discarded for the final calculations. A similar procedure, taking into account the slope variation of the curve "Gas production (NL) *vs.* Time (h)", as well as the H_2 flow rate, was applied when analyzing the results of the measurement campaign carried out in Grenoble.

The Quantum Efficiency for methane production is the product of the amount of CH_4 (n_{CH_4}) with the number of electrons required to transform CO_2 into CH_4, ($N_e = 8$),

divided by the number of incidents photons reaching the active area of the IPEC cells $(N_{ph} \times A)$.

$$QE_{CH_4} = \frac{N_e \times n_{CH_4}(mol)}{N_{ph}(mol.m^{-2}) \times A\ (m^2)}$$

To define the efficiency of the device we express the solar to fuel yield as the ratio of the chemical energy produced and the incident solar energy E_{sun}.

$$STF_{\text{GHI}} = \frac{Chemical\ energy}{Solar\ energy} = \frac{mol_{fuel\ produced} \times HHV_{fuel\ produced}\ (J.mol^{-1})}{E_{sun}(Wh.m^{-2}) * A\ (m^2) * 3600(J.Wh^{-1})}$$

The total higher heating value of the produced fuel is derived from the following equations:

$$HHV_{fuel\ produced} = HHV_{CH_4} \times X_{CH_4} + HHV_{H_2} \times X_{H_2}$$

HHV is the higher heating value corresponding to 890,800 J/mol for the green methane and to 285,667 J/mol for the unreacted hydrogen.

X_{CH_4} and X_{H_2} are respectively the volume fractions of methane and hydrogen in the gas at the reactor outlet.

Acknowledgments

This work was partly supported by Carnot Energies du Futur, the Agence Nationale de la Recherche (ANR) for projects Labex ARCANE and CBH-EUR-GS (ANR-17-EURE-0003), the DRF-Impulsion program and the ECC inflexion program of the Fundamental Research Division of CEA, and by the Carbon Circular Economy Program of the Energies Division of CEA. The authors thank Hervé Bercegol for his continous support during the project, Frédéric Fouda-Onana and Nicolas Guillet (LITEN) for their advices on PEM cells, Bertrand Chandez and Frédéric Vidal (LITEN), Michel Boujard and Eric Delamadeleine (IRIG) and the Tandem Cells Laboratory at CEA LITEN at INES for their technical support, as well as local organization team of the *Horizon Prize Grand Finale* at JRC Ispra for their welcome and for providing the irradiation data.

Authors contributions

Conceptualization: M.M., J.-M.B., C.C., V.A. and S.C.; Formal analysis: A.R.A.M., G.C., M.M., J.-M.B., A.M., G.C., S.C. and V.A.; Investigation: A.M., J.F., R.V., G.C., and A.R.A.M.; Writing – Original draft: A.R.A.M., G.C., M.M., J.-M.B. and S.C.; Writing – Review & Editing: A.R.A.M., C.C., M.M., S.C. and V.A.; Supervision: C.C., M.M., V.A. and S.C.

Declaration of interests

Some of the authors filed two patent applications:

- Pellat, M., Roux, G., Charton, S., Maragno, A. R. A., Photoelectrochemical converter for producing dihydrogne WO 2023057374. (2023).

- Pellat, M., Roux, G., Artero, V., Charton, S., Maragno, A. R. A., Matheron, M., Photoelectrochemical converter for producing dihydrogen WO 2023057376. (2023).

References

1. Segev, G., Kibsgaard, J., Hahn, C., Xu, Z.J., Cheng, W.S., Deutsch, T.G., Xiang, C., Zhang, J.Z., Hammarström, L., Nocera, D.G., et al. (2022). The 2022 solar fuels roadmap. J. Phys. D. Appl. Phys. *55*, 323003. https://doi.org/10.1088/1361-6463/ac6f97.

2. Nishiyama, H., Yamada, T., Nakabayashi, M., Maehara, Y., Yamaguchi, M., Kuromiya, Y., Tokudome, H., Akiyama, S., Watanabe, T., Narushima, R., et al. (2021). Photocatalytic solar hydrogen production from water on a 100 m2-scale. Nature *598*, 304–307. 10.1038/s41586-021-03907-3.

3. Andrei, V., Ucoski, G.M., Pornrungroj, C., Uswachoke, C., Wang, Q., Achilleos, D.S., Kasap, H., Sokol, K.P., Jagt, R.A., Lu, H., et al. (2022). Floating perovskite-BiVO4 devices for scalable solar fuel production. Nature *608*, 518–522. 10.1038/s41586-022-04978-6.

4. Larrazábal, G.O., Martín, A.J., and Pérez-Ramírez, J. (2017). Building Blocks for High Performance in Electrocatalytic CO2 Reduction: Materials, Optimization Strategies, and Device Engineering. J. Phys. Chem. Lett. *8*, 3933–3944. 10.1021/ACS.JPCLETT.7B01380.

5. Rönsch, S., Schneider, J., Matthischke, S., Schlüter, M., Götz, M., Lefebvre, J., Prabhakaran, P., and Bajohr, S. (2016). Review on methanation - From fundamentals to current projects. Fuel *166*, 276–296. 10.1016/j.fuel.2015.10.111.

6. Frontera, P., Macario, A., Ferraro, M., Antonucci, P., Louis, B., Wang, Q., and Pereira, M.M. (2017). Supported Catalysts for CO2 Methanation: A Review. Catalysts *7*. 10.3390/catal7020059.

7. Hren, R., Vujanović, A., Van Fan, Y., Klemeš, J.J., Krajnc, D., and Čuček, L. (2023). Hydrogen production, storage and transport for renewable energy and chemicals: An environmental footprint assessment. Renew. Sustain. Energy Rev. *173*, 113113. 10.1016/j.rser.2022.113113.

8. Sayama, K., and Miseki, Y. (2014). Research and development of solar hydrogen production. Synth. English Ed. *7*, 79–91. 10.5571/syntheng.7.79.

9. Ardo, S., Fernandez Rivas, D., Modestino, M.A., Schulze Greiving, V., Abdi, F.F., Alarcon Llado, E., Artero, V., Ayers, K., Battaglia, C., Becker, J.-P., et al. (2018). Pathways to electrochemical solar-hydrogen technologies. Energy Environ. Sci *11*, 2768. 10.1039/c7ee03639f.

10. Detz, R.J., Reek, J.N.H., and Van Der Zwaan, B.C.C. (2018). The future of solar fuels: when could they become competitive? Energy Environ. Sci *11*, 1653. 10.1039/c8ee00111a.

11. Walter, M.G., Warren, E.L., McKone, J.R., Boettcher, S.W., Mi, Q., Santori, E.A., and Lewis, N.S. (2010). Solar water splitting cells. Chem. Rev. *110*, 6446–6473. 10.1021/cr1002326.

12. Maragno, A.R.A., Morozan, A., Fize, J., Artero, V., Charton, S., and Matheron, M. (2024). Thermally integrated photoelectrochemical devices with perovskite / silicon tandem solar cells : a modular approach for scalable direct water splitting. ChemRxiv,

1–24. https://doi.org/10.26434/chemrxiv-2024-xc4rq.

13. Tembhurne, S., Nandjou, F., and Haussener, S. (2019). A thermally synergistic photo-electrochemical hydrogen generator operating under concentrated solar irradiation. Nat. Energy *4*, 399–407. 10.1038/s41560-019-0373-7.

14. Lourenço, A.C., Reis-Machado, A.S., Fortunato, E., Martins, R., and Mendes, M.J. (2020). Sunlight-driven CO2-to-fuel conversion: Exploring thermal and electrical coupling between photovoltaic and electrochemical systems for optimum solar-methane production. Mater. Today Energy *17*, 100425. 10.1016/j.mtener.2020.100425.

15. Jia, J., Seitz, L.C., Benck, J.D., Huo, Y., Chen, Y., Ng, J.W.D., Bilir, T., Harris, J.S., and Jaramillo, T.F. (2016). Solar water splitting by photovoltaic-electrolysis with a solar-to-hydrogen efficiency over 30%. Nat. Commun. *7*, 1–6. 10.1038/ncomms13237.

16. Yamaguchi, S., Watanabe, K., Minegishi, T., and Sugiyama, M. (2023). Solar to hydrogen efficiency of 28.2% under natural sunlight achieved by a combination of five-junction concentrator photovoltaic modules and electrolysis cells. Sustain. Energy Fuels, 1377–1381. 10.1039/d2se01754g.

17. Fehr, A.M.K., Agrawal, A., Mandani, F., Conrad, C.L., Jiang, Q., Park, S.Y., Alley, O., Li, B., Sidhik, S., Metcalf, I., et al. (2023). Integrated halide perovskite photoelectrochemical cells with solar-driven water-splitting efficiency of 20.8%. Nat. Commun. *14*, 3797. 10.1038/s41467-023-39290-y.

18. Tembhurne, S., and Haussener, S. (2016). Integrated Photo-Electrochemical Solar Fuel Generators under Concentrated Irradiation. J. Electrochem. Soc. *163*, H999–H1007. 10.1149/2.0321610jes.

19. Kim, J.H., Hansora, D., Sharma, P., Jang, J.W., and Lee, J.S. (2019). Toward practical solar hydrogen production-an artificial photosynthetic leaf-to-farm challenge. Chem. Soc. Rev. *48*, 1908–1971. 10.1039/c8cs00699g.

20. Aydin, E., Allen, T.G., De Bastiani, M., Xu, L., Ávila, J., Salvador, M., Kerschaver, E. Van, and De Wolf, S. (2020). Interplay between temperature and bandgap energies on the outdoor performance of perovskite/silicon tandem solar cells. Nat. Energy *5*, 851–859. 10.1038/s41560-020-00687-4.

21. Chisholm, G., Kitson, P.J., Kirkaldy, N.D., Bloor, L.G., and Cronin, L. (2014). 3D printed flow plates for the electrolysis of water: An economic and adaptable approach to device manufacture. Energy Environ. Sci. *7*, 3026–3032. 10.1039/c4ee01426j.

22. Yang, G., Mo, J., Kang, Z., Dohrmann, Y., List, F.A., Green, J.B., Babu, S.S., and Zhang, F.Y. (2018). Fully printed and integrated electrolyzer cells with additive manufacturing for high-efficiency water splitting. Appl. Energy *215*, 202–210. 10.1016/j.apenergy.2018.02.001.

23. Charton, S., Janvier, J., Rivalier, P., Chaînet, E., and Caire, J.-P. (2010). Hybrid sulfur cycle for H2 production: A sensitivity study of the electrolysis step in a filter-press cell. Int. J. Hydrogen Energy *35*, 1537–1547. 10.1016/j.ijhydene.2009.12.046.

24. Goyal, N., Zhou, Z., and Karimi, I.A. (2016). Metabolic processes of Methanococcus maripaludis and potential applications. Microb. Cell Fact. *15*, 107. 10.1186/s12934-016-0500-0.

25. Cwicklinski, G., Miras, R., Pérard, J., Rinaldi, C., Darrouzet, E., and Cavazza, C. (2024). Development of a CO2-biomethanation reactor for producing methane from green H2. Sustain. Energy Fuels *8*, 1068–1076. 10.1039/d3se01550e.

26. Jud, G., Schneider, K., and Bachofen, R. (1997). The role of hydrogen mass transfer for the growth kinetics of Methanobacterium thermoautotrophicum in batch and chemostat cultures. J. Ind. Microbiol. Biotechnol. *19*, 246–251. 10.1038/sj.jim.2900461.

27. Thema, M., Weidlich, T., Hörl, M., Bellack, A., Mörs, F., Hackl, F., Kohlmayer, M., Gleich, J., Stabenau, C., Trabold, T., et al. (2019). Biological CO2-Methanation: An Approach to Standardization. Energies *12*, 1670. 10.3390/en12091670.

28. Datta, K., Branco, B., Zhao, Y., Zardetto, V., Phung, N., Bracesco, A., Mazzarella, L., Wienk, M.M., Creatore, M., Isabella, O., et al. (2023). Efficient Continuous Light-Driven Electrochemical Water Splitting Enabled by Monolithic Perovskite-Silicon Tandem Photovoltaics. Adv. Mater. Technol. *8*, 2201131. 10.1002/admt.202201131.

29. Holmes-Gentle, I., Tembhurne, S., Suter, C., and Haussener, S. (2023). Kilowatt-scale solar hydrogen production system using a concentrated integrated photoelectrochemical device. Nat. Energy *8*, 586–596. 10.1038/s41560-023-01247-2.

30. Pehlivan, İ.B., Oscarsson, J., Qiu, Z., Stolt, L., Edoff, M., and Edvinsson, T. (2021). NiMoV and NiO-based catalysts for efficient solar-driven water splitting using thermally integrated photovoltaics in a scalable approach. iScience *24*, 101910. 10.1016/j.isci.2020.101910.

31. Wang, Y., Sharma, A., Duong, T., Arandiyan, H., Zhao, T., Zhang, D., Su, Z., Garbrecht, M., Beck, F.J., Karuturi, S., et al. (2021). Direct Solar Hydrogen Generation at 20% Efficiency Using Low-Cost Materials. Adv. Energy Mater. *11*, 1–11. 10.1002/aenm.202101053.

32. Chen, Z., Wang, T., Liu, B., Cheng, D., Hu, C., Zhang, G., Zhu, W., Wang, H., Zhao, Z.J., and Gong, J. (2020). Grain-Boundary-Rich Copper for Efficient Solar-Driven Electrochemical CO2 Reduction to Ethylene and Ethanol. J. Am. Chem. Soc. *142*, 6878–6883. 10.1021/jacs.0c00971.

33. Gurudayal, Beeman, J.W., Bullock, J., Wang, H., Eichhorn, J., Towle, C., Javey, A., Toma, F.M., Mathews, N., and Ager, J.W. (2019). Si photocathode with Ag-supported dendritic Cu catalyst for CO2 reduction. Energy Environ. Sci. *12*, 1068–1077. 10.1039/c8ee03547d.

34. Jia, Q., Tanabe, S., and Waki, I. (2018). Direct Gas-phase CO2 Reduction for Solar Methane Generation Using a Gas Diffusion Electrode with a BiVO4:Mo and a Cu-In-Se Photoanode. Chem. Lett. *47*, 436–439. 10.1246/cl.171094.

35. Sekimoto, T., Hashiba, H., Shinagawa, S., Uetake, Y., Deguchi, M., Yotsuhashi, S., and Ohkawa, K. (2016). Wireless InGaN – Si / Pt device for photo- electrochemical water splitting. Jpn. J. Appl. Phys. *55*, 088004. 10.7567/JJAP.55.088004.

36. Gurudayal, Bullock, J., Srankó, D.F., Towle, C.M., Lum, Y., Hettick, M., Scott, M.C., Javey, A., and Ager, J. (2017). Efficient solar-driven electrochemical CO2 reduction to hydrocarbons and oxygenates. Energy Environ. Sci. *10*, 2222–2230. 10.1039/c7ee01764b.

37. Huan, T.N., Dalla Corte, D.A., Lamaison, S., Karapinar, D., Lutz, L., Menguy, N., Foldyna, M., Turren-Cruz, S.H., Hagfeldt, A., Bella, F., et al. (2019). Low-cost high-efficiency system for solar-driven conversion of CO2 to hydrocarbons. Proc. Natl. Acad. Sci. U. S. A. *116*, 9735–9740. 10.1073/pnas.1815412116.

38. Ren, D., Loo, N.W.X., Gong, L., and Yeo, B.S. (2017). Continuous Production of Ethylene from Carbon Dioxide and Water Using Intermittent Sunlight. ACS Sustain. Chem. Eng. *5*, 9191–9199. 10.1021/acssuschemeng.7b02110.

39. Creissen, C.E., and Fontecave, M. (2021). Solar-Driven Electrochemical CO2 Reduction with Heterogeneous Catalysts. Adv. Energy Mater. *11*, 1–12. 10.1002/aenm.202002652.

40. Rahaman, M., Andrei, V., Wright, D., Lam, E., Pornrungroj, C., Bhattacharjee, S., Pichler, C.M., Greer, H.F., Baumberg, J.J., and Reisner, E. (2023). Solar-driven liquid multi-carbon fuel production using a standalone perovskite–BiVO4 artificial leaf. Nat. Energy *8*, 629–638. 10.1038/s41560-023-01262-3.

41. Zoller, S., Koepf, E., Nizamian, D., Stephan, M., Patané, A., Haueter, P., Romero, M., González-Aguilar, J., Lieftink, D., de Wit, E., et al. (2022). A solar tower fuel plant for the thermochemical production of kerosene from H2O and CO2. Joule *6*, 1606–1616. 10.1016/j.joule.2022.06.012.

42. Kistler, T.A., Zeng, G., Young, J.L., Weng, L.C., Aldridge, C., Wyatt, K., Steiner, M.A., Solorzano, O., Houle, F.A., Toma, F.M., et al. (2020). Emergent Degradation Phenomena Demonstrated on Resilient, Flexible, and Scalable Integrated Photoelectrochemical Cells. Adv. Energy Mater. *10*, 1–10. 10.1002/aenm.202002706.

43. Luo, G., and Angelidaki, I. (2012). Integrated biogas upgrading and hydrogen utilization in an anaerobic reactor containing enriched hydrogenotrophic methanogenic culture. Biotechnol. Bioeng. *109*, 2729–2736. 10.1002/bit.24557.

44. Murano, R., Maisano, N., Selvaggi, R., Pappalardo, G., and Pecorino, B. (2021). Critical issues and opportunities for producing biomethane in Italy. Energies *14*, 1–14. 10.3390/en14092431.

45. Babics, M., De Bastiani, M., Ugur, E., Xu, L., Bristow, H., Toniolo, F., Raja, W., Subbiah, A.S., Liu, J., Torres Merino, L. V., et al. (2023). One-year outdoor operation of monolithic perovskite/silicon tandem solar cells. Cell Reports Phys. Sci. *4*, 101280. 10.1016/j.xcrp.2023.101280.

46. McKone, J.R., Lewis, N.S., and Gray, H.B. (2014). Will solar-driven water-splitting devices see the light of day? Chem. Mater. *26*, 407–414. 10.1021/cm4021518.

47. Aydin, E., Ugur, E., Yildirim, B.K., Allen, T.G., Dally, P., Razzaq, A., Cao, F., Xu, L., Vishal, B., Yazmaciyan, A., et al. (2023). Enhanced optoelectronic coupling for perovskite/silicon tandem solar cells. Nature *623*, 732. 10.1038/s41586-023-06667-4.

48. James, B.D., Baum, G.N., J., P., and Baum K.N. (2009). Technoeconomic Analysis of Photoelectrochemical (PEC) Hydrogen Production 10.1023/A:1016025709833.

49. Andrei, V., Wang, Q., Uekert, T., Bhattacharjee, S., and Reisner, E. (2022). Solar Panel Technologies for Light-to-Chemical Conversion. Acc. Chem. Res. *55*, 3376–3386. 10.1021/ACS.ACCOUNTS.2C00477.